Power cycling testing with different load pulse durations

U.Scheuermann*, R.Schmidt*, P.Newman[†]

*SEMIKRON Elektronik GmbH & Co. KG, Sigmundstr. 200, 90419 Nürnberg, Germany, uwe.scheuermann@semikron.com,
[†]SEMIKRON Ltd., 9 Harforde Court, John Tate Road, Hertford SG13 7NW, United Kingdom, paul.newman@semikron.com

Keywords: Reliability, power modules, lifetime model, lifetime estimation

Abstract

For many applications, the impact on the component lifetime of temperature swings generated by low output frequency is of special interest. Therefore, active power cycling tests with a variation of load pulse duration were conducted. The requirements for the active power cycling test equipment related to load pulse durations down to 70ms will be discussed. The analysis of the test results leads to the proposal of a new empirical lifetime model for advanced power modules, which explicitly contains the impact of the load pulse duration. These reliability results will affect the design of advanced inverters with low frequency output currents.

1 Introduction

The generation, distribution and transformation of electrical energy is of prominent importance for modern societies. Power electronics is providing the technology to utilize electrical energy in the most efficient way for a multitude of different fields of application: exploitation of renewable energy sources, public and individual transport, as well as uninterruptible power supplies for server farms and data centers; all of which have gained some public attention lately, and are only the tip of the iceberg – our modern society is dependent on electrical energy.

Electrical engineers all over the world are working on the improvement of power electronic devices and components to increase the reliability and efficiency of power inverter systems. Classical power modules exposed to active power cycling are limited in lifetime by two main failure mechanisms: solder fatigue and wire bond degradation. Since any degradation in the thermal path from the chip to the heat-sink results in increasing thermal resistance and thus in growing junction temperatures of the devices, progress in power module design must first solve the problem of solder fatigue. The advanced architecture of the SKiM63/93 power module family is a 100% solder free design [1] where a diffusion silver sinter technology is applied for die attachment.

Based on experimental results of active power cycling tests on the 1200V SKiM63 power module with a wide spread of test parameters, a new empirical lifetime model was derived. Since only Al wire bond failures are found as end-of-life mechanisms in these tests, this model can be considered as a lifetime model for aluminum wire bonds. However, the sequence of layer materials and thicknesses in the module architecture could impact the lifetime model coefficients, so that a general applicability of this model must be validated before use.

2 SKiM63 power module design

Figure 1 shows the module design of the SKiM63/93 power module family which was introduced in 2008 [1]. The exploded view shows from bottom to top: the Al_2O_3 DBC substrate with the silicon IGBTs and diodes attached by Ag diffusion sintering (the 300µm Al wire bonds are not shown in this image), the housing which aligns all elements, the spring contacts for control signals, the multiple contact Plus, Minus and AC terminals and finally, the elastic spring pad and rigid pressure plate on the top.
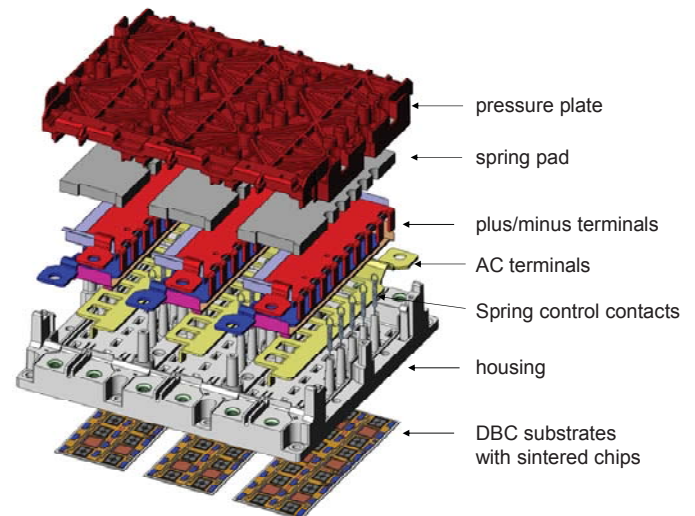

Fig. 1: Advanced power module design - SKiM93.

Mounting the module on a heat-sink establishes all thermal and electrical contacts simultaneously.

3 Active power cycling

Active power cycling testing is the most important endurance test for power modules. Constant DC current pulses are conducted by the devices under test (DUTs). The on-state losses dissipated in the devices thus generate a sequence of temperature swings. The parameters monitored continuously during the power cycling test are the on-state voltage drop of the devices at the end of the heating phase just before the load

current is turned off, and the (maximum) junction temperatures of the DUTs are determined by the $V_{CE}(T)$ method shortly after the load pulse is turned off [2]. By recording both parameters continuously, degradation effects can be monitored during the test.

There are several possibilities for a control strategy in the presence of degradation effects. One possible strategy is to adapt the operational parameters with the goal to keep the junction temperature swing constant. This strategy is often discussed in academia. However in real applications, such measures to compensate for parameter degradation are typically not implemented. A comparison of different control strategies has shown, that compensation strategies can over-estimate the lifetime by a factor of 3 [3]. Therefore, all tests discussed in this paper have been conducted with a constant t_{on}/t_{off} control without any compensation for degradation. The temperature swing was determined after the parameters had stabilized over 100 cycles in the initial phase of the test.

It should be emphasized, that the philosophy of testing should comply with the concept of lifetime estimation, if lifetime prediction based on mission profiles is the goal. Using the same measurement techniques (e.g. $V_{CE}(T)$ method for thermal resistance measurement and power cycling test setup) and characterizing systems in its initial state without degradation allows to derive lifetime models which can be extrapolated for application-specific mission profiles.

Fig. 2: Active power cycling test equipment.

Figure 2 shows a state-of-the-art power cycling equipment used for the power cycling investigation presented here. A constant DC current up to 600A is switched between two branches of the equipment ensuring constant load is presented to the power supply. Each branch can host 4 DUTs which are electrically connected in series but cooled by parallel cooling paths. Each DUT is a phase leg consisting of two switches in

series. The gate voltage can be controlled for each switch individually; this allows compensation for small variations in thermal resistance and on-state voltage between different switches. As a consequence of this design, t_{on} and t_{off} are complementary in the two branches, so that typically both values are selected equal. To avoid load changes on the DC constant current supply, the voltage drop should be comparable in both branches of the test equipment.

A liquid cooling system extracts the dissipated heat from the DUTs. The cooling liquid temperature can be adjusted in a wide range (20°C to 85°C) to investigate the impact of the medium junction temperature on the module lifetime. Special power cycling equipment with boosted heating/cooling capability can extend this range from -20°C to 100°C. The coolant flow can be continuous or clocked, i.e., turned off during the heating phase and turned on during the cooling phase.

For load pulse durations of 1s and above, the equipment can be controlled by software on a high level platform such as LabVIEW. For load pulses below 1s the control technique had to be improved. A special interface card with an internal clock signal was installed to switch the current between the branches independent of the high level software. The high level software only counts the cycles and initiates a measurement of on-state voltage drop and maximum junction temperature every 20 cycles, which reduces the data transfer rate as well as the data volume. Also, clocked water flow is not possible for short load pulses, so that these tests were performed with continuous coolant flow.

To achieve a targeted temperature swing with short load pulses of 100ms and below, high DC currents are required. This also results in a considerable average power for the condition $t_{on}=t_{off}$. The cooling capability of the power cycling equipment was not sufficient to cool a complete phase leg to the desired junction temperature level. Therefore, the power cycling tests with a load pulse duration of 70ms were performed on a single switch only.
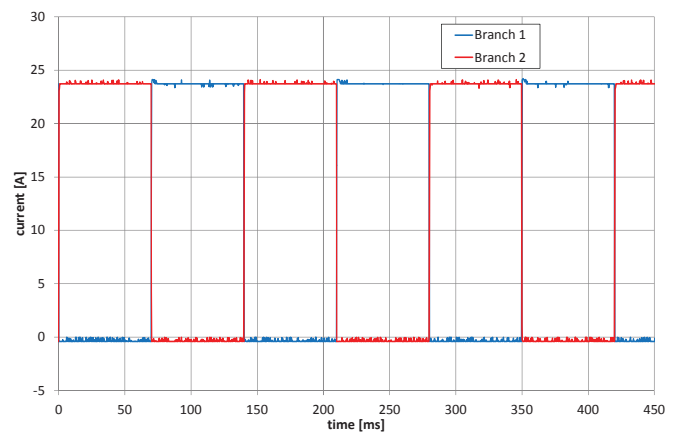

Fig. 3: DC current of 25A switched between two branches with $t_{on}=t_{off}$=70ms.

Figure 3 shows the current wave form switched between the two branches for load pulses of 70ms. The wave forms exhibit a perfect square shape without over-voltages at turn-

2

on or turn-off. This high quality of the wave form is important for power cycling tests with short load pulses.

4 The power cycling test matrix

For the new lifetime model, 97 power cycling tests were evaluated. Nine tests were performed on diodes and 88 tests on IGBTs in the SKiM63 package. A wide spread of parameters was realized to obtain a good experimental basis for the lifetime model deduction.

Figure 4 shows the variation of the medium temperature T_{jm} as a function of ΔT_j. Tests with negative coolant temperatures have been performed to realize medium junction temperatures in a range between 32.5°C and 122°C.

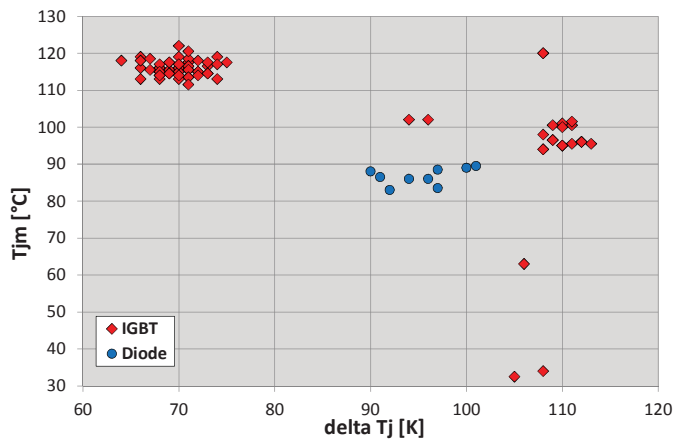Fig. 4: Variation of medium junction temperature T_{jm} versus temperature swing ΔT_j.

Figure 5 shows the variation of the wire bond aspect ratio ar as a function of ΔT_j. The aspect ratio, i.e., the ratio of loop height divided by the distance between two adjacent wire bond stitches, is a design parameter and is selected as 0.31 for the standard SKiM63 package. However, it was of interest to the authors to investigate the impact of wire bond geometry on the lifetime in active power cycling tests. Therefore, the aspect ratio was varied between 0.19 and 0.42 in the power cycling test matrix.
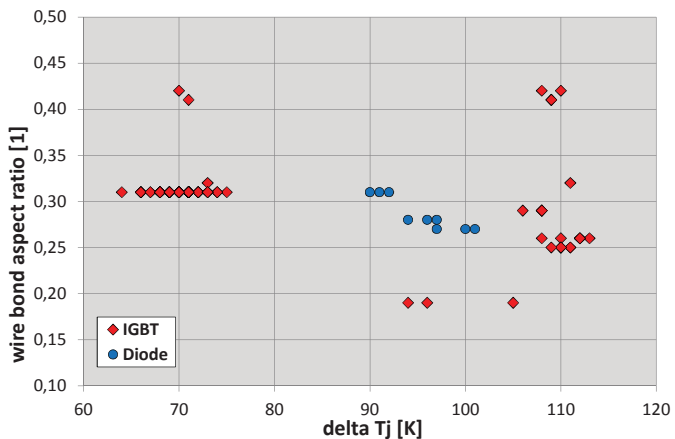
Fig. 5: Variation of wire bond aspect ratio ar versus temperature swing ΔT_j.

Figure 6 shows the variation of the load pulse duration t_{on} as a function of ΔT_j. The dependence on this parameter was a special focus of the test program and almost three orders of magnitude in t_{on} were achieved between 70ms and 63s pulse duration.
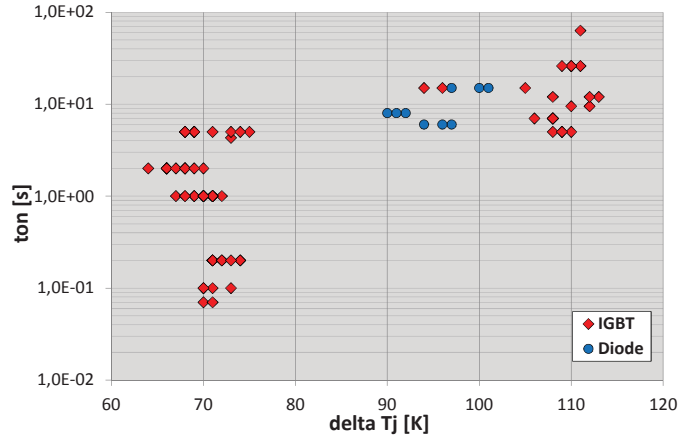
Fig. 6: Variation of load pulse duration t_{on} versus temperature swing ΔT_j.

Figure 7 shows the range of cycles to failure accomplished as a function of ΔT_j between $3.1 \cdot 10^4$ and $7.7 \cdot 10^6$. The failure analysis performed after the EoL tests always showed wire bond failures. Since no solder layer was implemented in the architecture, effects of solder fatigue were completely eliminated. No sign of degradation was observed in the Ag diffusion sintered die attachment.

For the wire bond failures, two different failure modes were observed: Wire bond lift-off and wire bond heel cracks. Wire bond heel cracks were only found in modules bonded with small wire bond aspect ratios (≤ 0.2) sometimes accompanied also by wire bond lift-off. For larger ar, no heel cracks could be detected; the failure mode was pure wire bond lift-off.
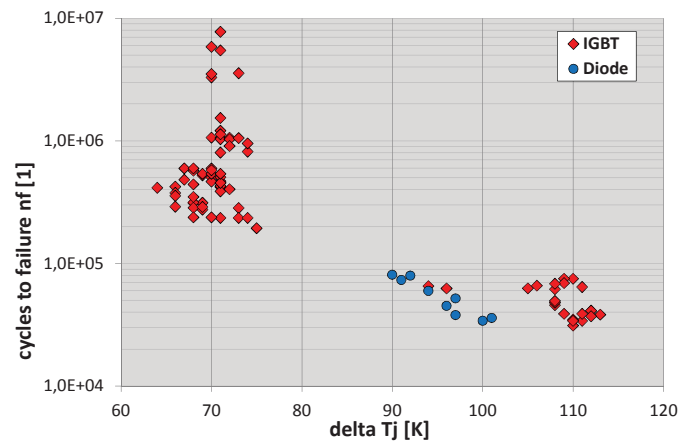
Fig. 7: Cycles to failure nf in active power cycling test versus temperature swing ΔT_j.

3

5 The history of lifetime models

In the early days of power electronic modules, power cycling tests were only performed until a specified number of cycles was reached at a single qualification condition. In order to extrapolate the results of accelerated power cycling tests to operational conditions, this single test point strategy was replaced by end-of-life (EoL) testing at different temperature swings ΔT_j. In the mid-1990s, a comprehensive test program was conducted in the LESIT project, which established the first universal lifetime model for classical power modules [4]. The experimental results demonstrated, that the medium temperature T_{jm} has to be taken into account in addition to the dependence on the temperature swing ΔT_j. The impact of the medium temperature of the swing was described by an Arrhenius factor.

The failure modes in classical power modules were studied thoroughly by many groups and are well described. The dominant physical EoL failure modes are solder fatigue and wire bond lift-off and/or wire bond heel cracking.

A significant effort was invested in the progress of packaging technologies to enhance the reliability of the classical modules design on the one hand. On the other hand, improvements of test equipment has led to a wider base of power cycling test results. The CIPS 2008 lifetime model [5] extended the list of model parameters by the load pulse duration t_{on}, the current per bond stitch I, the chip voltage class V_C and the wire bond diameter d. The model was based on more than 150 power cycling test results on several different package designs.

In modern power systems, lifetime prediction becomes more and more important. Detailed lifetime models are necessary to estimate the power component lifetime. With the advent of interconnection technologies with increased reliability, improved lifetime models are required to exploit the advantages of this progress.

However it should be emphasized, that lifetime models are always derived from accelerated power cycling test data and then extrapolated to field conditions with lifetimes of 20 years and more. These models cannot be validated for field operation conditions; even if one would accept test durations of 20 years, the results would be only of historical interest due to the technological progress.

6 The SKiM63/93 lifetime model

A phenomenological approach was selected for the new SKiM63 lifetime model. The already discussed LESIT model was taken as a base line and additional factors have been added to reflect the results of supplemental investigations on wire bond failures (see Eq. 1)

$$n_f = A \cdot \Delta T_j^{\alpha} \cdot \exp\left(\frac{E_a}{k_B \cdot T_{jm}}\right) \cdot ar^{\beta_1 \cdot \Delta T_j + \beta_0} \cdot \left(\frac{C + t_{on}^{\gamma}}{C+1}\right) \cdot f_{Diode} \quad (1)$$

The factor A is a constant scaling factor. A Coffin-Manson factor describes the impact of the temperature swing ΔT_j and an Arrhenius term the dependence on the medium junction temperature T_{jm} as in the LESIT model with both temperature values given in Kelvin. While the exponent α is in the same range as in the LESIT model, the activation energy E_a of the Arrhenius term is much smaller than in the LESIT model. Closer investigations on this observation have shown that the dependence on the medium temperature is much less pronounced for wire bond degradation than for solder fatigue [6].

The dependence on the wire bond aspect ratio ar is implemented by a power law with the exponent being a linear function of the temperature swing ΔT_j. This approach reflects the result of a previous investigation on wire bond failures in base plate modules [7]. The comparison of power cycling lifetime for soldered and sintered die attachment confirmed, that the improvement of wire bond geometry by higher loops, which was predicted from mechanical stress tests [8], can only be exploited if solder fatigue is eliminated. A major finding of this investigation was, that the increase of lifetime for larger aspect ratios was more pronounced at lower temperature swings. The significant impact of wire bond geometry on lifetime was also confirmed by [9].

The next factor expresses the dependence on the load pulse duration t_{on} (in seconds). The functional dependence of this factor is based on a theoretical assumption: For a medium load pulse duration, stress is imposed in the interfaces by the generated temperature gradient and plastic deformation increases the strain. If the pulse duration is reduced, the time for plastic deformation is reduced as well and the resulting degradation decreases. If the pulse length is increased, maximum plastic deformation is achieved and a stationary situation is reached. The factor, which is normalized to a pulse duration of 1s, is reflecting this assumption: For negative values of the exponent γ this factor approaches a constant value for growing t_{on}, while it increases exponentially for shorter pulse duration.

The last factor is describing different power cycling lifetime results for IGBT and diodes. It is unity for IGBTs and the value f_{Diode} for diodes as given in the parameter list in Table 1.

Parameter	Unit	Value
A	[1]	$3.4368 \cdot 10^{14}$
α	[1]	-4.923
E_a	[eV]	$6.606 \cdot 10^{-2}$
β_1	[1/K]	$-9.012 \cdot 10^{-3}$
β_0	[1]	1.942
C	[1]	1.434
γ	[1]	-1.208
f_{Diode}	[1]	0.6204

k_B in Eq. 1 is the Boltzmann constant in eV/K.

Table 1: Lifetime model parameters for SKiM63/93.

A least square fit was performed on the complete set of 97 power cycling test results. The obtained model parameters are given in Table 1. For comparison of the model accuracy, all test data sets were sorted for the number of cycles to failure as predicted by the model. Figure 8 shows these sorted model

predictions along with the experimental results. As expected, the least square fit delivers an average prediction of the power cycling lifetime. As discussed in detail in [10], a quasi-statistical evaluation reveals a survival rate of 85% when the lifetime value of Eq. 1 is multiplied by a margin factor of 0.8.

Fig. 8: Experimental results compared to the predictions from the SKiM63 lifetime model.

In contrast to the CIPS 2008 model, the SKiM63 lifetime model contains no dependence on the wire bond diameter, because all tests were performed on modules bonded with 300μm Al wire bonds. Also, no impact of the current density per bond stitch could be confirmed. A least square fit with an additional current dependent factor did not result in a significant reduction of the sum of squared errors of the fit. However, the applied current in this investigation was always within the specified nominal data sheet value with a current density between 1.27A and 6.55A per bond stitch.

A voltage class dependent factor as in the CIPS 2008 model could also not be verified, because only 1200V IGBTs and diodes were used in experiment. However, if we compare the de-rating factor of the CIPS 2008 model for a 1200V CAL diode with 260μm thickness relative to a 1200V IGBT4 of 120μm thickness, the CIPS 2008 model predicts a factor of ~0.59 compared to the SKiM63 diode de-rating factor of ~0.62.

7 Impact of load pulse duration

The influence of the load pulse duration t_{on} was of special interest in this investigation. Several factors can be used to perform power cycling tests with comparable ΔT_j and different pulse duration: Changing the current magnitude, adjusting the gate voltage V_{GE} and varying the cooling conditions.

Figure 9 displays selected power cycling test results with a large variation of load pulse durations. The tests have been selected for smallest differences in the medium temperature T_{jm}. The detailed test parameters are collected in Table 2.

The cooling conditions were constant for all power cycling tests, however by changing the configuration of the test circuit (single IGBT switch or phase leg, i.e., two IGBT switches connected in series) the effective thermal capacity of

the heat-sink is altered. The gate voltage was adjusted to increase or decrease the losses produced by the constant load current. And the current itself was adapted to produce the desired combination of ΔT_j and t_{on}. It should be emphasized, that all test modules were bonded according to the series design and the current remained within the specification limits.
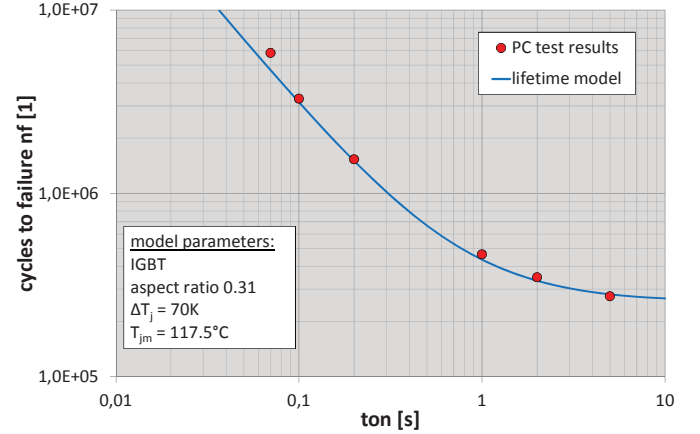

Fig. 9: Selected power cycling results compared to the estimation of the SKiM63 lifetime model.

Configuration	t_{on} [s]	V_{GE} [V]	I_{bs} [A]	ΔT_j [K]	T_{jm} [°C]
Single switch	0.07	13.2	6.55	70	122
Phase leg	0.1	13.5	5.99	70	113
Phase leg	0.2	14.6	5.37	71	113.5
Phase leg	1	15.3	3.99	70	119
Phase leg	2	15.0	3.75	68	115
Phase leg	5	17.8	3.80	69	115.5

all tests were performed on IGBTs with *ar* = 0.31.

Table 2: Test condition for selected power cycling results.

Inverter tests with output frequencies of 1Hz and 3Hz have confirmed the general trend, that increased lifetime is observed for operation at higher load pulse frequencies [11].

8 Conclusion

A new lifetime model is presented for the SKiM63/93 power module family. It is applicable to advanced power modules without base plates, Ag sintered die attachment and 300μm Al wire bonds. Since no solder interconnection is implemented in this model it could be considered as a basis for a general lifetime model of Al wire bonds. However, since the arrangement and material of layers in module design could have an impact on the wire bond stress, the general applicability must be validated for different architectures.

An important result is the explicit dependence of the lifetime on the load pulse duration and therefore on the output frequency of an inverter. This is especially important for all applications, where inverter input or output frequencies between 1 and 20Hz form a major contribution to the application-specific mission profile, e.g., gearless wind

generators with the dominant stress occurring just in this frequency range.

This explicit time dependence must be considered in the lifetime estimation process from mission profiles. Classical Rainflow algorithms do not take pulse lengths into account. However, an extension of these cycle-counting algorithms for time dependent lifetime models is possible.

References

[1] U.Scheuermann, P.Beckedahl: "The Road to the Next Generation Power Module – 100% Solder Free Design", *Proc. CIPS 2008, Nuremberg, ETG-Fachbericht* **111**, pp. 111-120.

[2] U.Scheuermann, R.Schmidt: "Investigations on the $V_{CE}(T)$-Method to Determine the Junction Temperature by Using the Chip Itself as Sensor", *Proc. PCIM Europe, CD-ROM, Nürnberg*, 2009.

[3] S.Schuler, U.Scheuermann: "Impact of Test Control Strategy on Power Cycling Lifetime", *Proc. PCIM Europe, paper 57*, pp. 355-360, (2010).

[4] M.Held, P.Jacob, G.Nicoletti, P.Scacco, M.H.Poech: "Fast Power Cycling Test for IGBT Modules in Traction Application", *Proc. Power Conversion and Drive Systems* 1997, pp. 425-430.

[5] R.Bayerer, T.Herrmann, T.Licht, J.Lutz, M.Feller: "Model for Power Cycling lifetime of IGBT Modules – various factors influencing lifetime", *Proc. CIPS 2008, ETG-Fachbericht* **111**, pp. 37-42.

[6] R.Schmidt, F.Zeyß, U.Scheuermann: "Impact of Absolute Junction Temperature on Power Cycling Lifetime", *Proc. EPE 2013 ECCE Europe*.

[7] U.Scheuermann, R.Schmidt: "Impact of Solder Fatigue on Module Lifetime in Power Cycling Tests", *Proc. EPE*, 2011.

[8] S.Ramminger, N.Seliger, G.Wachutka: "Reliability Model for Al Wire Bonds Subjected to Heel Crack Failures", *Microelectronics Reliability* **40** (2000), pp. 1521-1525.

[9] S.Hartmann, E.Özkol: "Bond wire lifetime model based on temperature dependent yield strength", *Proc. PCIM Europe* 2012, pp. 494-501.

[10] U.Scheuermann, R.Schmidt: "A New Lifetime Model for Advanced Power Modules with Sintered Chips and Optimized Al Wire Bonds", *Proc. PCIM Europe* 2013, pp. 810-817.

[11] U.Scheuermann, R.Schmidt: "Impact of load pulse duration on power cycling lifetime of Al wire bonds", *Microelectronics Reliability* **53** (2013), pp. 1687–1691.